R. & M. No. 2929
(12,623 14,671)
A.R.C. Technical Report

MINISTRY OF SUPPLY

AERONAUTICAL RESEARCH COUNCIL
REPORTS AND MEMORANDA

Tests Concerning Novel Designs of Blades for Axial Compressors

PART I. BLADES DESIGNED FOR INCREASED WORK AT ROOT AND TIP

PART II. BLADES DESIGNED TO OPERATE IN A PARABOLIC AXIAL VELOCITY DISTRIBUTION

By

S. J. Andrews, R. A. Jeffs and E. L. Hartley

LONDON: HER MAJESTY'S STATIONERY OFFICE
1956
PRICE 6*s.* 6*d.* NET

Tests Concerning Novel Designs of Blades for Axial Compressors

PART I. BLADES DESIGNED FOR INCREASED WORK AT ROOT AND TIP

PART II. BLADES DESIGNED TO OPERATE IN A PARABOLIC AXIAL VELOCITY DISTRIBUTION

By

S. J. ANDREWS, R. A. JEFFS and E. L. HARTLEY

COMMUNICATED BY THE PRINCIPAL DIRECTOR OF SCIENTIFIC RESEARCH (AIR), MINISTRY OF SUPPLY

Reports and Memoranda No. 2929*

October, 1951

Summary.—Investigation of the flow between the blade rows in a research compressor with conventional Half-Vortex blades have shown a rapid stage-to-stage build-up of the annulus boundary layer. The axial velocity distribution under these conditions bears no resemblance to the straight-line distribution which is usually assumed in design so the incidence angles at both root and tip probably give rise to considerable secondary losses.

Two sets of blades were designed therefore, with the object of minimising these effects. The first set was designed with an increased work input at the root and tip of the blades in order to re-energise the boundary layer and prevent axial-velocity profile deterioration. The second set was designed using as a design assumption a mathematical approximation to the axial-velocity profiles found experimentally at various stages in a conventional compressor.

The results obtained from low-speed tests of the first set of blades show that although the boundary-layer thickness was considerably reduced, this was achieved only at the expense of 2 per cent in maximum efficiency as compared with conventional blades. The drop in efficiency is attributed to the stator blade rows which stall at incidences well below the design value, but the effect is probably not uniquely associated with variable work done.

The blades designed for a variable axial-velocity profile also failed to give an improved performance. The maximum efficiency was 3 per cent below that of the equivalent conventional blades and the axial-velocity profile instead of remaining approximately as assumed, deteriorated still further.

It is considered that designing for a poor axial-velocity profile is probably wrong in principle. The Variable Work Done blades, however, would almost certainly have succeeded in producing an axial velocity substantially constant over the greater part of the annulus if the work had been symmetrically distributed about the mean radius with a ratio of mean to minimum work of about $1 \cdot 1$. Under these circumstances it is likely that there would have been a reduction in secondary losses and an increase in efficiency.

1. *Introduction.*—In designing an axial compressor of medium or high hub-tip ratio it is usually assumed that the axial velocity is either constant across the annulus or has an almost straight-line variation from blade root to blade tip. In practice, however, the axial-velocity profile produced in the compressor probably has a maximum value near the mean diameter with very thick boundary layers on the annulus walls. This difference between design and actual conditions means that a substantial part of the blade height may be operating at incidences very different from the design incidence.

* N.G.T.E. Memorandum M.54, received 5th October, 1949.
N.G.T.E. Report R.104, received 26th February, 1952.

To offset these effects and produce a compressor which has reasonable gas incidence angles over more of the blade height represents a possible source of improved performance by reduction of secondary losses. The two ways of tackling the problem of increasing the efficiency in this way which are investigated are, either to prevent the deterioration of the velocity profile and therefore the adverse effects it produces, or alternatively, assume that the velocity profile will deteriorate, and design blades which will operate successfully in such a profile.

The method adopted to prevent the deterioration of the axial-velocity profile is to design the blades for increased work at root and tip and reduced work at the mean diameter. In this way, the boundary layer will be re-energised in each stage and the velocity profile maintained substantially the same throughout the compressor. It is for this reason that the six stages of Variable Work Done blades are all identical since the object is to maintain rather than to change a state of affairs.

A rather different principle is adopted in designing blades specifically to operate in, for instance, a parabolic velocity profile. The stages are designed in pairs to suit the velocity profile found at that station in a conventional compressor. In this instance, therefore, the first two stages are designed for uniform axial velocity across the annulus, the second two for a parabolic profile and the third two for a parabolic profile with a greater ratio of maximum to mean axial velocity.

To produce truly comparable results, the two sets of blades are designed to give the same mean temperature rise per stage at the same value of mean-flow coefficient. The results and analysis of these two tests are presented separately in Parts I and II of the report and in each part the reference comparison is with the performance of the compressor with a set of Free-Vortex blades having the same design temperature rise and flow coefficient.

PART I

Blades Designed for Increased Work at Root and Tip

2. *The Compressor.*—2.1. *Blade Design.*—The tests described in Ref. 1 showed that the axial-velocity profile which developed in the compressor had a maximum value nearer the inner diameter than the outer diameter. The variation of work done over the blade height, of the blades designed for increased work at root and tip was chosen therefore to be that illustrated in Fig. 3. The work input is greater at the root and tip than at mean diameter but the excess work is weighted in favour of the outer diameter. The other design assumptions are listed and the resulting blade angles of the Variable Work Done (V.W.D.) blades and of the corresponding conventional Free-Vortex blades with similar design assumptions are shown in this figure and in Fig. 2.

The compression ratio of the compressor at 1,500 r.p.m., the speed at which most of the tests were done, is so low that no correction to the single-stage design need be made to compensate for the density change through six stages.

2.2. *Description of the Compressor and Test Equipment.*—A general description of the compressor is given in Ref. 4 and will not be repeated here. It is sufficient to say that the compressor has a constant rotor and casing diameter with a diameter ratio of $0 \cdot 75$. Throughout the tests the rotational speed was 1,500 r.p.m. giving a blade speed of 114 ft per second at the mean diameter and a Reynolds number based on this speed of $6 \cdot 2 \times 10^4$.

Other relevant factors which have not been previously mentioned will be briefly described. The surface finish of the blades for instance is anodised giving a smoothness equal to that of a polished metal surface. The roots of both rotor and stator blade have fillets of approximately 0·12 in. radius on to the circular-root boss. This boss has a diameter of 0·75 in. so that the fillet extends only over the centre portion of the blade. Details of the relative position of blade rows, traverse planes and other instruments are shown in Fig. 1. The rotor tip clearance shown is a nominal value only, being the clearance if the rotor and stator casings were completely co-axial. In fact the number of spigots on the stator case permits a small amount of relative movement and this together with the flexibility of the stator half-rings means that the tip clearance at any one point cannot be defined to nearer than 0·025 in. $\pm$0·020 in.

2.3. *Blade Accuracy.*—To establish the accuracy of blade form and setting a typical V.W.D. stator blade was chosen and the following details are applicable to that blade.

	Design values			Measured values		
Radius r (in.)	7·5	8·75	9·85	7·5	8·75	9·85
Camber θ	39·0	29·0	40·0	38·8	29·4	38·4
Chord c	1·06	1·10	1·14	1·05	1·09	1·13
$\frac{\text{Thickness}}{\text{Chord}}$ t/c	0·10	0·11	0·12	0·096	0·113	0·136
Relative stagger $-\zeta$ (deg)	+0·9°	0	−2·4°	+1·4°	0	−2·2°

The tolerance in mean-diameter blade-setting angle allowed when the V.W.D. blades were mounted in the compressor was 0·1 deg. The Free-Vortex blades however which were not checked as rigorously may have local stagger variations of up to 0·5 deg. Blade setting is accomplished with a straight edge laid on the concave surface of the blade, if therefore there is an error in blade form then the stagger angle as properly defined may be in error. This will in practically all cases not exceed 0·1 deg.

From the table it can be seen that the camber angle is within 0·4 deg except at the stator root where the fillet tends to alter the effective value even at a distance of 0·15 in. from the boss.

2.4. *Calibration of Instruments.*—Both the claw-type pitot yawmeter and the static-pressure tube were calibrated in a nozzle and gave satisfactory results, the zero of the yawmeter was repeatable within 0·2 deg from the beginning to the end of the tests on the V.W.D. blades and the static-pressure tube was found insensitive to yaw angles of up to $\pm$4·0 deg from the stream direction.

2.5. *Torque Measurement.*—The torque reaction on the casing of the driving motor is measured by a balance at the end of a torque arm. It has been found preferable to obtain the zero reading of the balance by allowing the dynamometer to rotate at several very low speeds and then extrapolate the curve to zero speed. This eliminates for instance the error arising from forces transmitted through the brush gear. In addition the vibration when running reduces the possibility of slight sticking in the trunnion bearings. The repeatability of this zero is within 0·1 lb in a reading of 20 lb at 1,500 r.p.m.

2.6. *Test Procedure.*—To obtain the overall characteristics for both Free-Vortex and V.W.D. compressors six stages of blades were tested at a spacing of about two-thirds of the mean chord.

The detailed flow investigation for the V.W.D. compressor was also carried out with this form of build but the detailed investigation of the flow through the Free-Vortex blades was done on a four-stage build of the compressor with $1\frac{1}{2}$-chord spacing between the blade rows.

3. *Overall and Stage Characteristics.*—The overall characteristics of the two compressors are shown in Fig. 5 and are plotted in terms of efficiency, temperature coefficient, and pressure coefficient.

The two sets of curves are very similar in form but the maximum efficiency of the V.W.D. is about 2 per cent below the Free-Vortex compressor. No great significance should be attached to the coincidence of the temperature rise curves because as shown later the V.W.D. stator root sections are largely stalled. The two compressors have in fact very different working conditions relative to the design values. Neither compressor achieves the design temperature rise and the overall work done factors at the design flows are 0·81 for the Free-Vortex and 0·83 for the V.W.D. compared with the design value of 0·95.

The stage characteristics of the compressors shown in Fig. 6 are obtained from one static pressure tapping between each blade row. A common feature of the two sets is the slope of the curve for the first stage which is greater than that of the subsequent stages. This has been found to occur in other compressors including that reported in Ref. 3 and in tests on the 'water' compressor at N.G.T.E. as yet unpublished. The sets of characteristics have a somewhat random relative position in terms of pressure rise for a particular flow. This is more marked in the V.W.D. compressor and is probably due to variation in pressure round the compressor annulus.

4. *Blade Performance in Detail.*—4.1. *Axial-Velocity Distribution.*—As shown in Fig. 3 the V.W.D. blading is designed for a greater amount of work at the outer diameter than at the inner diameter. This has a considerable bearing on the axial-velocity distribution and gives some guide to the order of work variation required to retain a substantially uniform axial velocity through a multi-stage compressor.

From the general form of the curves shown in Figs. 7 and 8 it is evident that the Free-Vortex compressor suffers a rapid build up in boundary layer at both root and tip, so that at the fourth stage the profile is roughly parabolic. On the other hand the V.W.D. blading imposes a velocity profile with a peak at the outer diameter where the greatest work is done. This shape which is established in passing through the first rotor blade row is maintained throughout the remaining stages. The boundary-layer thickness in this instance is small and does not increase.

Most compressors are designed assuming a constant axial velocity from root to tip of the blade. A velocity profile which has therefore a minimum deviation from this constant value also has the greatest possibility of small secondary losses. The velocity profiles of the Free-Vortex and W.V.D. blading are compared on this basis in Fig. 10b. The variation of the profile from the optimum is defined as the arithmetic mean distance of the velocity profile from the straight line representing the mean axial velocity. This expressed as a percentage of the mean axial velocity is the parameter plotted in the figure

$$\text{Profile Shape Parameter } \delta\frac{V_a}{\bar{V}_a} = \frac{\int_{r_I}^{r_O}[(1 - V_a/\bar{V}_a)_{V_a/\bar{V}_a < 1} \text{ or } (V_a/\bar{V}_a - 1)_{V_a/\bar{V}_a > 1}]\,dr}{r_O - r_I}\,.$$

The curves show that, in passing from behind the first rotor to the fifth stator the velocity profile produced by the V.W.D. blades is improved by a small amount. The profile produced by the Free-Vortex blades however, deteriorates rapidly and although considerably better than the V.W.D. after the first rotor, it is worse in all blade rows after the second-stage stator. In previous work the axial-velocity profile shape has been expressed in terms of the ratio of mean to maximum velocity. Curves in these terms are shown in Fig. 10a.

It is interesting to speculate what variation of work done would have given an almost constant velocity distribution. If the design work done variation had been symmetrical about the mean diameter, then it could have been either the existing variation in the outer half of the annulus and its mirror image in the inner half or similarly, with the variation in the inner half duplicated in the outer half. The ratio of mean to minimum work would have been $1 \cdot 14$ and $1 \cdot 06$ respectively. It is reasonable to estimate that a variation with a $1 \cdot 1$ ratio of mean to minimum work symmetrically distributed about the mean blade height would have given an almost constant axial-velocity distribution. This figure, although not generally applicable, is nevertheless a useful guide.

The results are encouraging in so far as a variation of design work done along the blade can enable the axial velocity to be kept near the design value over most of the annulus so that only a small proportion of the blade is working at high incidences.

4.2. *Gas Angles.*—Considering first the rotor blades of the two compressors. From Figs. 11 and 13 it is plain that the circumferential mean value of the outlet angles follow the same form of curve as the predicted values over the majority of the blade height. There is however a general increase in the deviation angle $(\alpha_2 - \beta_2)$ of $0 \cdot 5$ to $2 \cdot 5$ deg. The rotor deviation has therefore been under estimated by about $1 \cdot 5$ deg at incidences equal to and below the design value. No very accurate measurements of loss coefficient at each radius could be obtained but the shape of the curves as estimated from results is shown in Figs. 11 and 13.

The two loss peaks at root and tip are associated with the trailing vortices (Ref. 1).

The stator gas angles of both compressors show much larger departures from the design value, particularly at the outside diameter, (*see* Figs. 12 and 14). These figures show that the last two stages of the Free-Vortex compressor and all the traversed stages of the V.W.D. compressor have deviations much larger than those given by design rules even before the incidence has reached its design value. The stalling incidence as predicted from cascade tests, Ref. 2, is a further 5 deg above the design incidence. A similar effect occurs in the stators of the Half-Vortex blades tested in the same compressor and reported in Ref. 1, Figs. 15 and 16. The reason for the stalling at the stator outer diameter is not comprehended since firstly, if there is any radial flow of the blade boundary layer, it would be away from the outer diameter and secondly there is no relative movement of the annulus wall, as there is at the inner diameter. At higher values of V_a/U the incidences of course decrease and the deviation at the V.W.D. stator inner diameter decreases toward the design value, (*see* Fig. 14,) but at the outer diameter the outlet angle approaches the design value at a much lower rate.

The loss coefficients which are plotted for the V.W.D. stators Fig. 14 are reasonably accurate, probably within plus or minus 10 per cent. There is no concentration of high loss over the stalled parts of the blade but the mean value is high, indicating that the loss wake is more evenly distributed than the outlet angle figures would suggest. No reliable loss figures for the Free-Vortex stators are available so the probable shape only, is indicated by the dotted line.

5. *Work Done Factor.*—The true work done in a rotor blade row is obtained from the traverse results by integrating the angular momentum per second across the annulus and taking the difference of the integrals at inlet and outlet sections. This value is compared with that predicted

using design gas angles and velocities, but excluding any empirical coefficient. The ratio of the two gives the work done factor which in terms of measured quantities is

$$\Omega = \frac{\left[\int_{r_I}^{r_O} UV_{a2}^2 \tan\alpha_3\, r\, dr - \int_{r_I}^{r_O} UV_{a1}^2 \tan\alpha_0\, r\, dr\right]_{\text{actual}}}{\left[\int_{r_I}^{r_O} UV_{a2}^2 \tan\alpha_3\, r\, dr - \int_{r_I}^{r_O} UV_{a1}^2 \tan\alpha_0\, r\, dr\right]_{\text{design}}} .$$

The work done factors for the various stages of the two compressors are shown in Fig. 15. The points for the V.W.D. compressor are plotted at the inter-stage positions because the temperature rise is calculated from the difference in angular momentum integrals after the rotor and stator of a particular stage, instead of before and after the rotor of that stage, which is the more usual method. This is necessitated by the compressor traverse ring arrangement.

The work done factors are high in the first stage and reduced in subsequent stages but there is no steady fall as found in Ref. 1. This is understandable in the case of the V.W.D. compressor where steady flow is quickly set up and maintained, but it is not obvious why it should be so in the Free-Vortex design. The second stage of this compressor has a low work done, as a result of the high deviation from the first-stage stator. This high deviation may be only apparent and due in fact to an error in blade setting, but there is no corresponding drop in the pressure characteristic for the stage to confirm this. The values of work factor are however reasonable and are considered representative of the stage performance in a multi-stage machine.

PART II

Blades Designed to Operate in a Parabolic Axial-Velocity Distribution

6. *Blade Design.*—The earlier tests Ref. 1 showed that a first approximation to the shape of the axial-velocity distribution in the compressor could be made by considering it as a parabola symmetrical about the mean diameter. It must be pointed out that this does not give zero velocity at the walls of the compressor annulus, but the reduction in velocity towards the walls is in fair agreement with measured profiles up to a point very close to the boundary. These measured velocity profiles showed that as the distribution deteriorated through the compressor, it could be represented by a series of parabolae of which the ratio of the mean axial velocity to the axial velocity at the mean diameter $\bar{V}_a/V_{a\,m/d}$, was successively reduced.

Two sets of blades were therefore designed to work at nominal incidences in axial-velocity distributions given by parabolas of which this ratio had the values 0·9 and 0·8. These two parabolic designs, subsequently called Variable Axial Profile, or V.A.P. blades, retained all the design assumptions of the conventional Free-Vortex design with the exception of the constant axial velocity criterion.

Full details of the procedure adopted in the design are given in Appendix II, and the resultant blade details are shown in Fig. 4.

6.1. *Compressor Assembly.*—For the overall tests on the six stages of blades, the compressor was assembled with an axial clearance between successive blade rows of approximately two-thirds of a mean chord. The assembly of the compressor in this form is shown in Fig. 1. Two sets of blades were tested with this build. Firstly, six stages of the conventional blades were examined and then six stages comprising two stages of the conventional blades, followed by two stages of V.A.P. 0·9 blades, followed by two stages of V.A.P. 0·8 blades. Constant speed characteristics of efficiency pressure rise and temperature rise have been measured over the speed range of 300 r.p.m. to 1,800 r.p.m.

For the detailed traversing tests, the assembly of the compressor was as in Ref. 1, *i.e.*, four stages of blades arranged at approximately $1\frac{1}{2}$ blade chords axial spacing, with provision for the traversing of instruments before and after each blade row. Using this arrangement, four stages of conventional blades were tested, and then four stages comprising two stages of conventional blades followed by two stages of V.A.P. 0·9 blades. This latter asesmbly was thus equivalent to the first four stages of the second six-stage build. Traverses were made with pitot, static pressure and yawmeter tubes at 1,500 r.p.m. at two values of the flow coefficient, one near the design point and one near the surge point.

Traverses were also made after the six-stage rotor row in the second six-stage build, showing the nature of the flow after passage through the V.A.P. 0·8 blades.

7. *Overall Characteristics.*—The overall performance of the two different six-stage arrangements are shown plotted in terms of non-dimensional coefficients in Fig. 5. These characteristics were measured at 1,500 r.p.m., which gave a Reynolds number based on blade speed of $6 \cdot 2 \times 10^4$. This, as may be seen from Fig. 16, is just clear of the most disturbing effects of Reynolds number on the work done.

The most obvious feature of Fig. 5 is the similarity between performance curves of the Free-Vortex and V.A.P. blades. The work done characteristic is a little higher and the efficiency about 3 per cent lower in the working range but the shape of the curves is similar in every respect. This is quite remarkable, for although the mean performance was designed to be the same the blade angles at mean diameter and root and tip are very different.

8. *Blade Performance in Detail.*—8.1. *Axial Velocity Distribution.*—Fig. 9 shows the results of the detailed traversing which was carried out as explained in section 6.1. It will be seen that the axial velocity distribution as such, Fig. 9, and as represented by the parameter $\bar{V}_a/V_{a\,\max}$, Fig. 10, deteriorated on passage through the conventional blades in a manner similar to that reported in Ref. 1. As may be expected, the rate of deterioration was much greater near the surge point than near the design point, where the aerodynamic loading on the blades was appreciably smaller. The deterioration caused by the V.A.P. blades was, however, considerably greater than that caused by the conventional blades at the same station along the compressor at both values of the flow coefficient at which traverses were made. The traverses after the sixth-stage rotor row of the second six-stage build showed that the V.A.P. 0·8 blades had a similar adverse effect on the velocity distribution.

The tests on the conventional blades, together with the tests reported earlier on a Half-Vortex design of blades, showed that if a conventional design is operated with an approximately uniform axial-velocity distribution, then that distribution will deteriorate rapidly in the first rows of the blades, the rate of deterioration falling off on passage through successive rows. The results of these tests on V.A.P. blades suggested that this statement should be amplified to say that any blade design which follows the conventional method of design or the method adopted for the V.A.P. blading will show this same development of the axial-velocity distribution from the design distribution.

9. *Effect of Reynolds Number on Performance.*—The constant speed characteristics obtained from the two six-stage assemblies have been plotted in a similar manner to those shown in Fig. 5. The values of the temperature rise coefficient, isentropic efficiency and pressure rise coefficient at the design value of the flow coefficient ($V_a/U = 0 \cdot 667$) have then been plotted against the Reynolds number of the flow, which is defined as:—

$$\text{Reynolds number} = \frac{\text{Blade speed} \times \text{blade chord}}{\text{Kinematic viscosity of ambient air}} .$$

The curves showing the variation of compressor performance with change of Reynolds number are shown in Fig. 16. Of these, the most reliable are those showing the variation of the pressure rise coefficient. These curves illustrate the considerably better performance of the conventional blades over the range of Reynolds number which was covered by these tests. The curves may be seen to follow the same general pattern and the major difference may be explained by the somewhat higher critical Reynolds number range for the V.A.P. blading. This critical range occurs where there is a transition between two different parts of the curve and may be seen for these two builds of the compressor to be about 3×10^4.

Extrapolation of these curves to the Reynolds numbers more commonly involved for axial compressors operating at or near ground level may be dangerous, as it may well happen that the two curves cross or at least meet.

The plotted values of isentropic efficiency should be regarded with some doubt when considering them as a measure of the performance of the blading alone. This is because a constant mechanical efficiency of 99 per cent was assumed in the calculation of all the values from the torque reaction of the dynamometer. While this may have given a fair estimate of the bearing losses, etc., at the higher speeds, it is probable that, at the lower end of the speed range, these losses consume a rather larger percentage of the input power. The efficiencies plotted are therefore, pessimistic at the low Reynolds numbers as a measure of pure blading efficiency. They may however be of the right order as an indication of the overall performance of a compressor, since any compressor operating at a lower Reynolds number then its design figure must suffer from a lower mechanical efficiency. The correction to be applied to the efficiency to allow for the mechanical efficiency will not be sufficient to flatten the curve completely.

While the absolute values of the efficiency may thus be in doubt, the difference between the efficiencies of the two builds are evident. Once more, the curve for the V.A.P. blades is of the same form as that for the conventional blades, but the critical Reynolds number range is reached at a somewhat higher value, resulting in considerably lower efficiencies over the whole range.

The temperature-rise coefficients shown in Fig. 16 are most seriously affected by a faulty estimation of mechanical efficiency since this coefficient is calculated from the relationship:—

$$\frac{2gJKp}{U^2} \cdot \Delta T_{\text{stage}} = \frac{\Delta P_{\text{stage}}}{\frac{1}{2}\rho U^2} \cdot \frac{1}{\eta} \, .$$

The considerable rise in the values at low Reynolds numbers must therefore be in doubt. As before, however, the difference between the curves is less suspect and the V.A.P. blading appears to give a higher work-done factor than the conventional blades at these low Reynolds numbers. This difference in work-done factors between the two builds disappears at higher Reynolds numbers, the two curves becoming coincident at approximately $0 \cdot 7 \times 10^5$.

---

10. *Conclusions* (*Parts I and II*).—Compressor blades can be designed with a work-done variation along their length so that the annulus boundary-layer air is re-energised and the axial-velocity profile is maintained substantially constant. In these tests this is achieved only at the expense of 2 per cent in maximum efficiency but the two effects are almost certainly not inseparable. In designing for more work at root and tip a ratio a maximum to mean work of $1 \cdot 1$ symmetrically distributed about the mean blade height is suggested as that needed to achieve an almost constant axial-velocity profile across the annulus.

The use of blades designed to operate in a parabolic axial velocity profile results in a drop in maximum efficiency of 3 per cent and a considerable deterioration of the axial-velocity profile beyond that caused by the conventional blades.

Of the two methods of attempting to improve the efficiency of the compressor by eliminating the secondary effects it is clear that the Variable Work Done blades show most promise. The aim in designing these blades is achieved in part and but for the stator blade stall the efficiency would have been greater.

Designing blades for a parabolic velocity profile in order to minimise the effects of that profile is probably wrong in principle since the secondary effects in this instance at least have merely superimposed themselves on the design conditions and produced a further deterioration of the profile.

It is suggested that the reason for the partial success of the Variable Work Done blades is that by designing in this way the energy can be restored to the air continuously at the position at which it is being dissipated by shed vortices and build up of the boundary layer.

REFERENCES

No.	*Author*	*Title, etc.*
1	D. G. Ainley and R. A. Jeffs	Analysis of the air flow through four stages of half-vortex blading in an axial compressor. R. & M. 2383. April, 1946.
2	A. D. S. Carter	The low-speed performance of related aerofoils in cascade. C.P. 29. September, 1949.
3	J. Bowden, R. H. Sabensky and W. D. Runnic	Theoretical and experimental investigation of an axial-flow compressor. Part 2. California Institute of Technology, Mechanical Engineering Laboratory 148962.
4	R. A. Jeffs	Description of the low speed experimental compressor No. 106. Power Jets Report R.1198, April, 1946. A.R.C. 10,832. (Unpublished.)

NOTATION

U	Blade speed
V_a	Axial velocity
V_m	Vector mean velocity
r	Radius
ΔT	Total temperature rise
ΔP	Total pressure rise
ρ	Gas density
s	Blade pitch
c	Blade chord
ε	Gas deflection angle
ζ	Blade stagger angle measured from axial direction
α	Gas angle measured from the axial direction
β	Blade angle measured from the axial direction
Ω	Work-done factor
$\bar{\omega}$	Mean total pressure loss
L	Lift per unit length of span
η	Efficiency

Suffices

0	After stator blade row of previous stage
1	Before rotor blade row
2	After rotor blade row
3	Before stator blade row
4	After stator blade row
m	Mean annulus diameter (except for V_m)
s	Compressor stage
I	Inner
O	Outer

APPENDIX I

Design of the Free-Vortex Compressor Blades

Assumptions V_a = constant

$U_m/V_a = 1\cdot5$

$\Delta T/\frac{1}{2}U_m^2 = 0\cdot8$ including work done factor

$\Omega = 0\cdot95$

Reaction = 50 per cent at $r/r_m = 0\cdot9$

$\tan\alpha_3 \propto 1/r$

$\tan\alpha_0 \propto 1/r$.

Then:—

$$\frac{\Delta T}{\frac{1}{2}U_m^2} = \frac{2V_a}{U_m}\cdot\frac{r}{r_m}(\tan\alpha_3 - \tan\alpha_0)\,\Omega$$

$$= 1\cdot27\,\frac{r}{r_m}(\tan\alpha_3 - \tan\alpha_0)$$

and at the radius of 50 per cent reaction, that is at $r/r_m = 0\cdot9$

$$(\tan\alpha_3 + \tan\alpha_0)_{r/r_m = 0\cdot9} = \frac{U_m}{V_a}\cdot\frac{r}{r_m} = 1\cdot35\,.$$

The design gas angles are therefore:

r (in.)	7·50		8·75		10·0
r/r_m	0·86	0·93	1·00	1·07	1·14
α_1	43·6	47·3	50·4	53·1	55·5
α_2	12·3	22·0	30·0	36·6	42·0
α_3	47·0	44·7	42·7	40·8	39·0
α_4	18·6	17·3	16·2	15·2	14·3

The rotor has 58 blades and the stator 60, so with blade chords of 1·14, 1·1 and 1·06 inches at root mean and tip diameters the blade angles are:—

	r/r_m	0·86	0·93	1·0	1·07	1·14
Rotor	β_1	43·9	47·4	49·5	51·1	52·3
	β_2	2·9	13·7	23·0	31·0	37·4
	θ	41·0	33·7	26·5	20·1	14·9
	s/c	0·712	0·787	0·862	0·942	1·020
Stator	β_3	47·5	45·0	42·4	40·0	37·5
	β_4	9·8	9·0	8·4	7·7	6·9
	θ	37·7	36·0	34·0	32·3	30·6
	s/c	0·740	0·788	0·833	0·876	0·918

The blades have C.4 base profiles on circular-arc camber-lines and the deviation rule used was $m\theta\sqrt{(s/c)}$ where m is a function of the stagger as given in Ref. 2.

APPENDIX II

Design of V.W.D. Compressor Blades

Assumptions $V_a = \text{constant}$

$$U_m/V_a = 1\cdot5$$

$$\overline{\Delta T}/\tfrac{1}{2}U_m^2 = 0\cdot786$$

$$\Omega = 0\cdot95\,.$$

Then:—

$$\frac{\Delta T}{\frac{1}{2}U_m^2} = \frac{2UV_a}{U_m^2}(\tan\alpha_3 - \tan\alpha_0)\Omega\,.$$

In an earlier design of the 106 compressor the axial velocities were lower at the outer diameter than the inner diameter (Fig. 11, Ref. 1) so the work done was made greater towards the tips of the rotor blades compared with their roots.

r (in.)	7·5		8·75		10·0
r/r_m	0·86	0·93	1·00	1·07	1·14
$\Delta T/\frac{1}{2}U_m^2$	0·798	0·716	0·723	0·834	0·991
α_1	43·6	47·5	50·4	53·2	55·6
α_2	11·5	25·6	33·1	35·9	35·6
α_3	45·6	42·9	41·7	41·8	42·1
α_4	16·1	17·8	17·8	15·6	12·3

The number of blades, the chord lengths and the design rules are the same as those for the Free-Vortex compressor

	r/r_m	0·86	0·93	1·0	1·07	1·14
Rotor	β_1	44·6	46·1	47·5	51·7	57·8
	β_2	2·1	19·1	28·0	29·7	25·8
	θ	42·5	27·0	20·0	22·0	32·0
	s/c	0·712	0·787	0·862	0·942	1·020
Stator	β_3	46·4	41·8	40·0	41·6	43·9
	β_4	7·4	10·8	11·0	7·6	1·9
	θ	39·0	31·0	29·0	34·0	42·0
	s/c	0·740	0·788	0·833	0·876	0·918

APPENDIX III

Design of V.A.P. Blades

Preliminary work on the effect of a parabolic axial velocity distribution on the air deflections required at the roots and tips of the blades to maintain constant work done at all radii showed that these could be made least severe by choosing the diameter of 50 per cent reaction for a Free-Vortex type of blade at approximately $0 \cdot 9 \times$ mean diameter. This value has accordingly been used in these calculations.

The details of the design are then as follows:—

(*a*) 50 per cent reaction at $0 \cdot 9 \times$ mean diameter

(*b*) $\dfrac{\text{Mean diameter blade speed}}{\text{Mean axial velocity}} = \dfrac{U_m}{\bar{V}_a} = 1 \cdot 5$

(*c*) Temperature rise coefficient, $\dfrac{2gJKp \,.\, \Delta T_{\text{stage}}}{U_m^{\,2}} = 0 \cdot 80$

(*d*) Work-done factor, $\Omega = 0 \cdot 95$

(*e*) Work done constant at all radii

(*f*) $r \,.\, Vw$ constant at all radii

(*g*) Velocity distribution parameter $= \dfrac{\text{Mean axial velocity, } \bar{V}_a}{\text{Axial velocity at mean diameter, } V_{am}}$

equal to $0 \cdot 9$ and $0 \cdot 8$ for V.A.P. blading, and equal to $1 \cdot 0$ for Free-Vortex blading.

Details of Calculations

at mean diameter, $r = 1$, $\dfrac{U_m}{V_a} = a$

$$\tan \alpha_2 = b$$

$$\tan \alpha_1 = d$$

$$\tan \alpha_3 = a - b$$

$$\tan \alpha_4 = a - d\,.$$

Then at any radius r, $\tan \alpha_4 = \dfrac{V_{am}}{V_a} \,.\, \dfrac{a - d}{r}$

$$\tan \alpha_3 = \frac{V_{am}}{V_a} \,.\, \frac{a - b}{r}$$

$$\tan \alpha_1 = \frac{V_{am}}{V_a} \left[ar - \frac{(a - d)}{r} \right]$$

$$\tan \alpha_2 = \frac{V_{am}}{V_a} \left[ar - \frac{(a - b)}{r} \right].$$

And at radius, R, of 50 per cent reaction,

$$\tan \alpha_4 = \tan \alpha_2$$

$$\frac{V_{am}}{V_a} \cdot \frac{a-d}{R} = \frac{V_{am}}{V_a}\left[aR - \frac{a-b}{R}\right]$$

Hence $$R = \left[2 - \left(\frac{b+d}{a}\right)\right]^{1/2} \quad \ldots \quad (1)$$

Work done (constant at all radii)

$$\Delta T_{\mathrm{tot}} = \frac{\Omega U V_a}{gJK_p}(\tan \alpha_1 - \tan \alpha_2) .$$

Therefore $$\frac{gJKp \,.\, \Delta T_{\mathrm{tot}}}{U_{M/D}^2} = \frac{V_{am}}{U_m}(\tan \alpha_1 - \tan \alpha_2)\,\Omega$$

$$= \frac{d-b}{a} \,.\, \Omega \,. \quad \ldots \quad (2)$$

From (1) and (2)

$$b = 0{\cdot}385a$$

$$d = 0{\cdot}806a .$$

Also $$a = 1{\cdot}5\,\underline{\overline{X}}$$

where $$\underline{\overline{X}} = \frac{\bar{V}_a}{V_{a\,\max}} .$$

The parabolic distribution of axial velocity is defined as:—

At radius r, $$V_a = \frac{\bar{V}_a}{\underline{\overline{X}}}\left[1 + 12\left(\frac{r-1}{r_o - r_I}\right)^2(\underline{\overline{X}} - 1)\right] .$$

These relationships are sufficient to give the air angles appropriate to each design. The numbers of blades, chords and design rules were the same as in the Free-Vortex design. The resultant blade details are shown in Fig. 4.

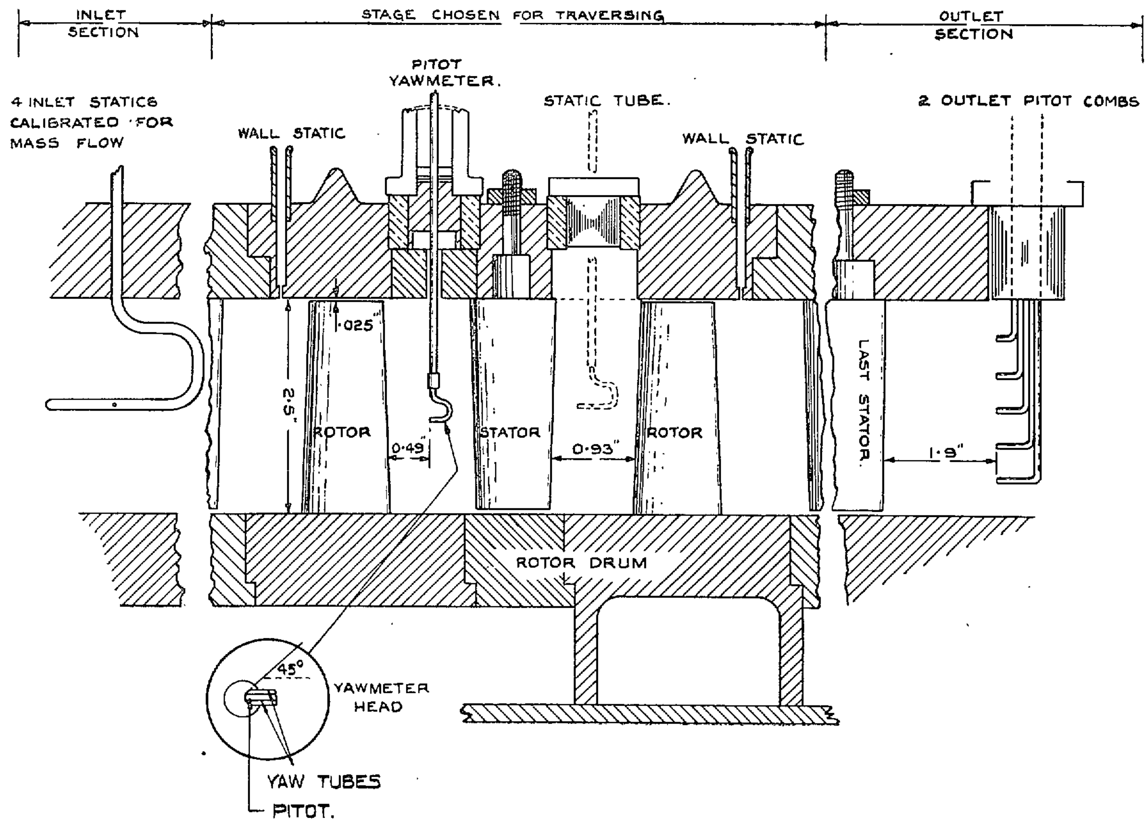

FIG. 1. Instrumentation of the 106 low-speed compressor.

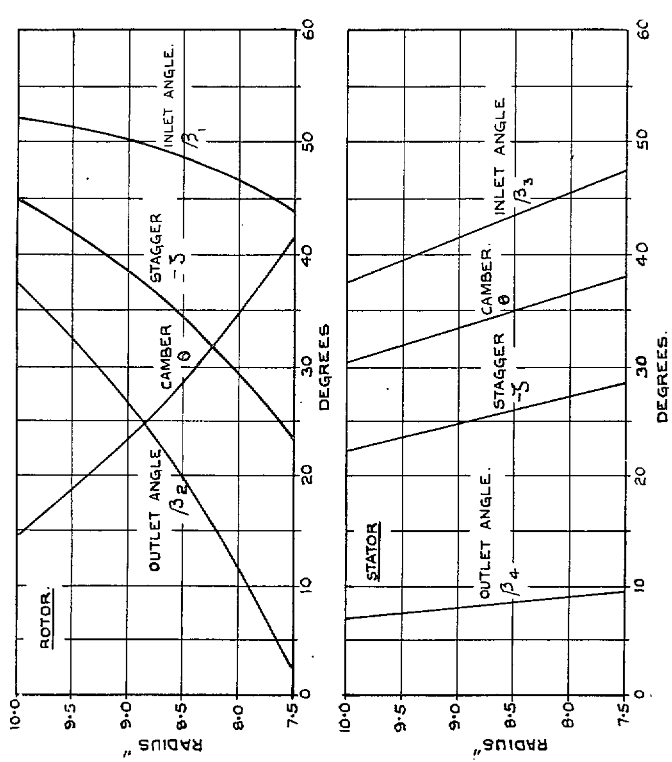

RADIUS "	7·50"		8·75"		10·0"	
	R	S	R	S	R	S
CHORD "	1·14	1·06	1·10	1·10	1·06	1·14
PITCH/CHORD	·711	·738	·862	·832	1·040	·918
THICKS/CHORD	·120	·100	·100	·110	·080	·120
NUMBER BLDS	58	60	58	60	58	60

DESIGN ASSUMPTIONS

$\Delta T / \tfrac{1}{2} U_m^2$ = ·800 (Ω = ·95)

U_m/V_a = 1·5

V_a = CONSTANT.

REACTION = 50% AT r = 7·9"

DEVIATION = $m\,\theta\sqrt{s/c}$

DEFLECTION = 0·9 ϵ MAX: (CASCADE.)

FIG. 2. Blade angles and data for Free-Vortex design.

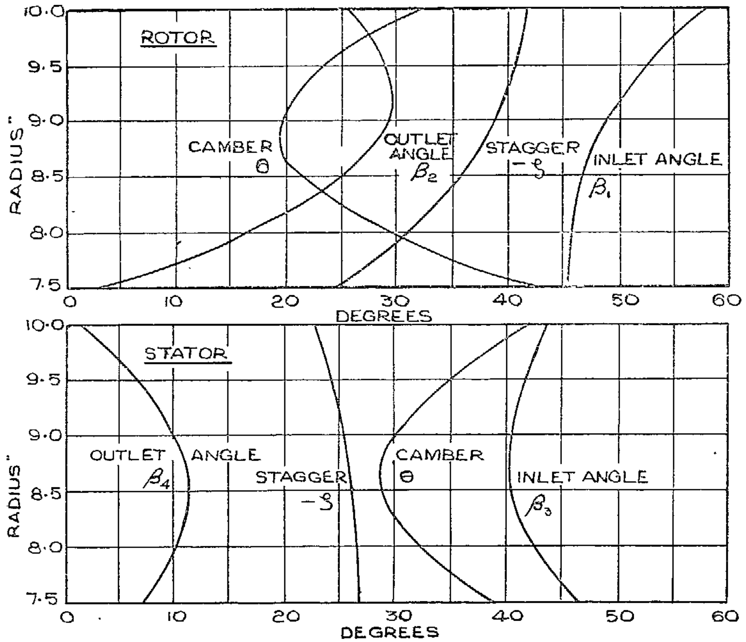

RADIUS"	7·50"		8·75"		10·0"	
	R	S	R	S	R	S
CHORD"	1·14	1·06	1·10	1·10	1·06	1·14
PITCH/CHORD	·711	·738	·862	·832	1·040	·918
THICKS/CHORD	·120	·100	·100	·110	·080	·120
NUMBER BLDS	58	60	58	60	58	60

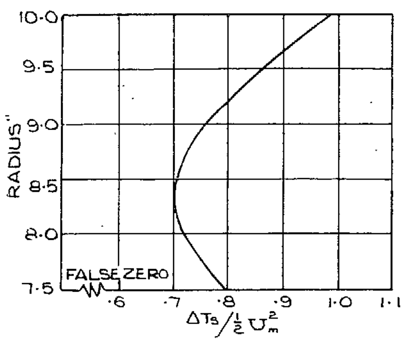

DESIGN ASSUMPTIONS

$\overline{\Delta T} / \frac{1}{2} U_m^2$ = ·790 $\Omega = 0{\cdot}95$

U_m / V_a = 1·5

V_a = CONSTANT

REACTION = 50% AT $r = 7{\cdot}6''$

DEVIATION = $m\theta\sqrt{s/c}$

DEFLECTION = 0·9 ε MAX (CASCADE)

FIG. 3. Blade angles and data for V.W.D. design.

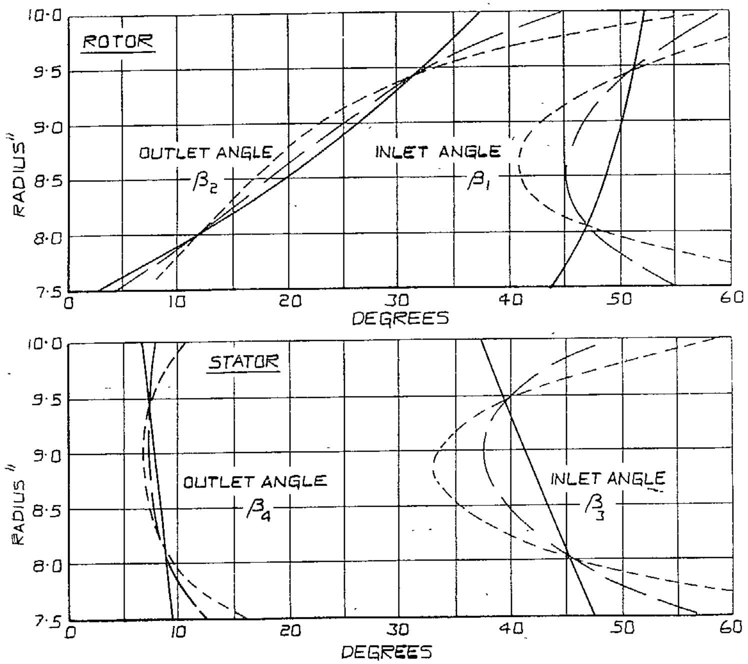

RADIUS"	7·50"		8·75"		10·0"	
	R	S	R	S	R	S
CHORD"	1·14	1·06	1·10	1·10	1·06	1·14
PITCH/CHORD	·711	·738	·862	·832	1·040	·918
THICKS/CHORD	·120	·100	·100	·110	·080	·120
NUMBER BLDS.	58	60	58	60	58	60

DESIGN ASSUMPTIONS

$\Delta T / \frac{1}{2} U_m^2$ = ·800 (Ω = ·95)

$U_m / \bar{V}_a$ = 1·5

V_a = PARABOLIC $\bar{V}_a / V_{am}$ {1·0 FREE VORTEX; 0·9 — — —; 0·8 - - - - - -}

REACTION = 50% AT $r = 7{\cdot}9''$

DEVIATION = $m\,\theta\sqrt{s/c}$

DEFLECTION = 0·9 ε MAX: (CASCADE)

FIG. 4. Blade angles and data for V.A.P. design.

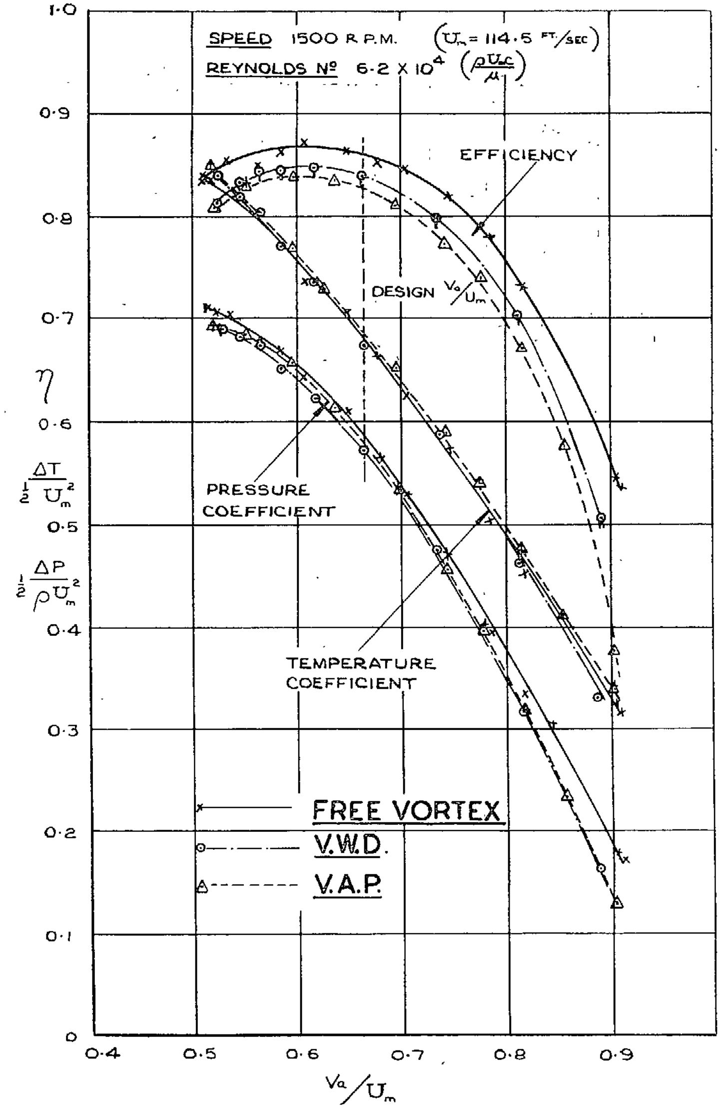

FIG. 5. Overall compressor characteristics.

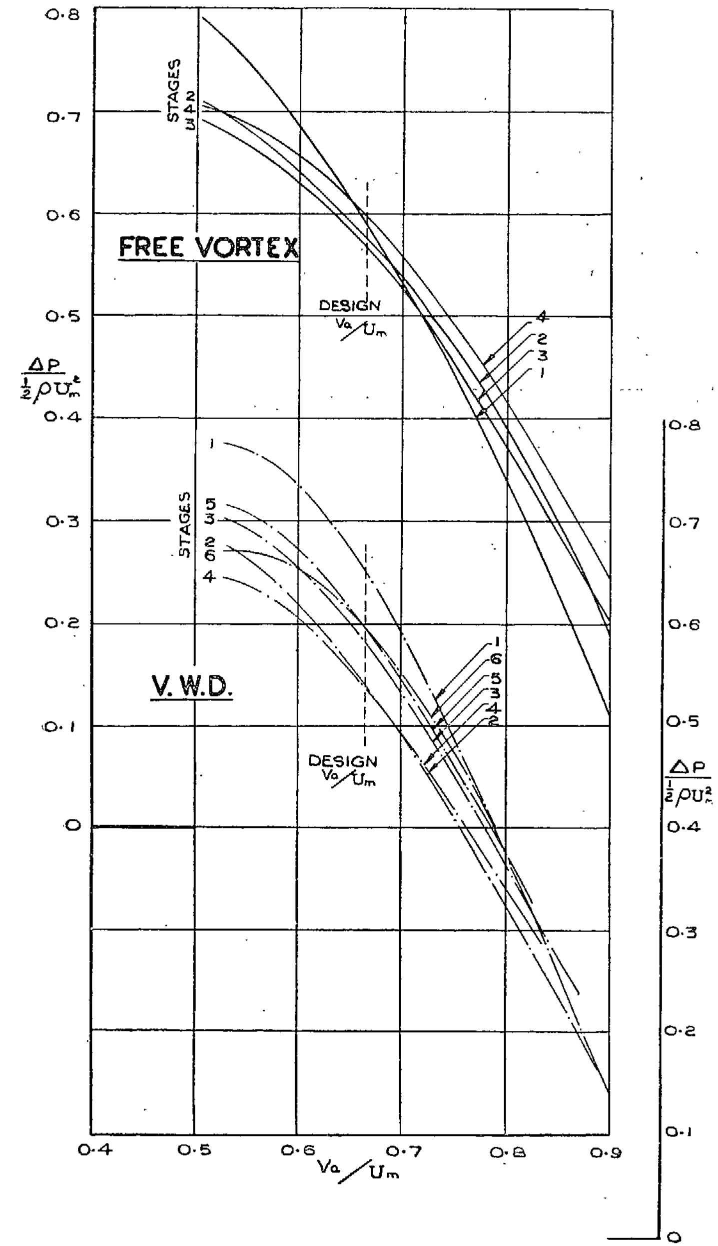

FIG. 6. Stage characteristics for Free-Vortex and V.W.D.

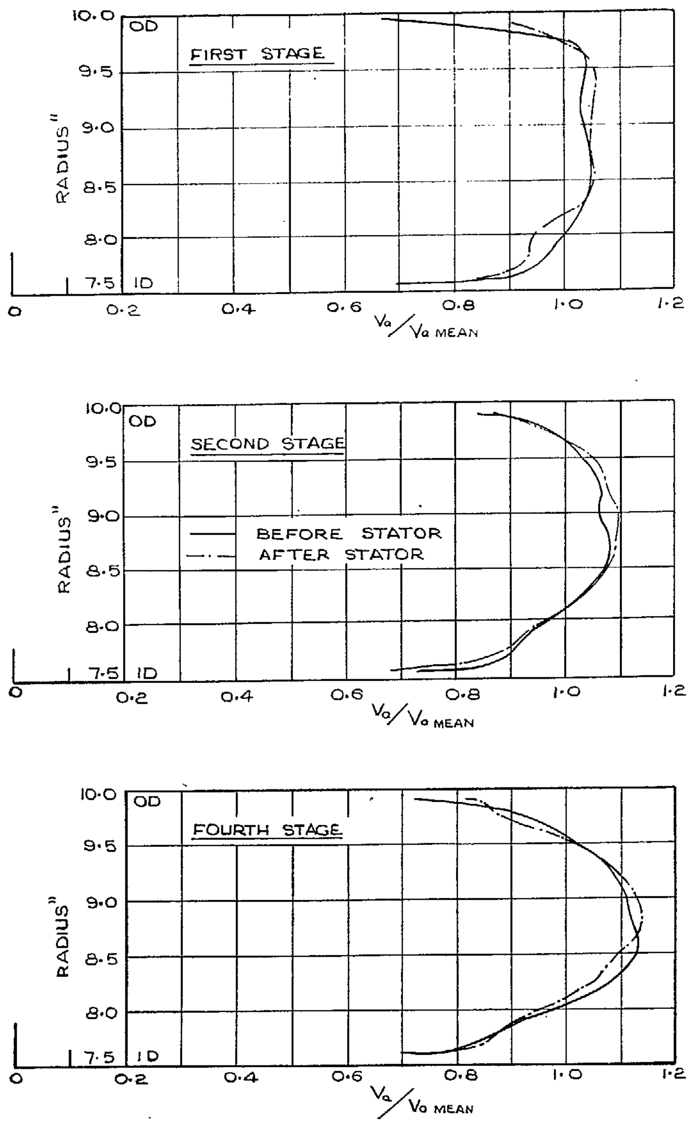

FIG. 7. Axial-velocity distribution of Free-Vortex design.

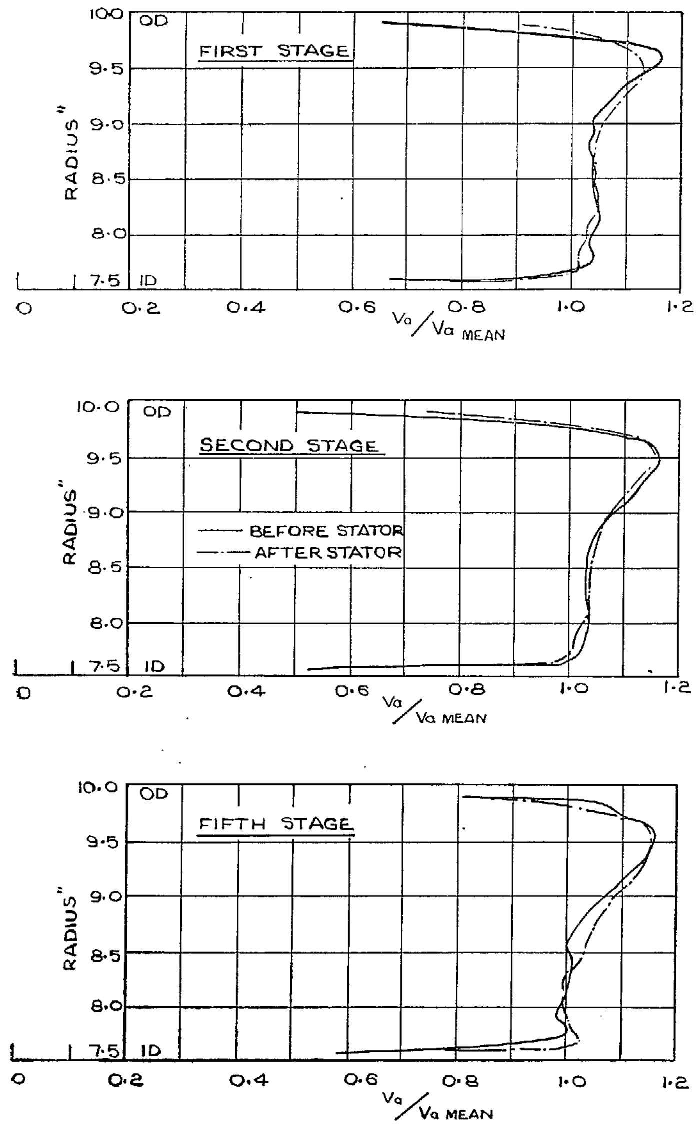

FIG. 8. Axial-velocity distribution of V.W.D. design.

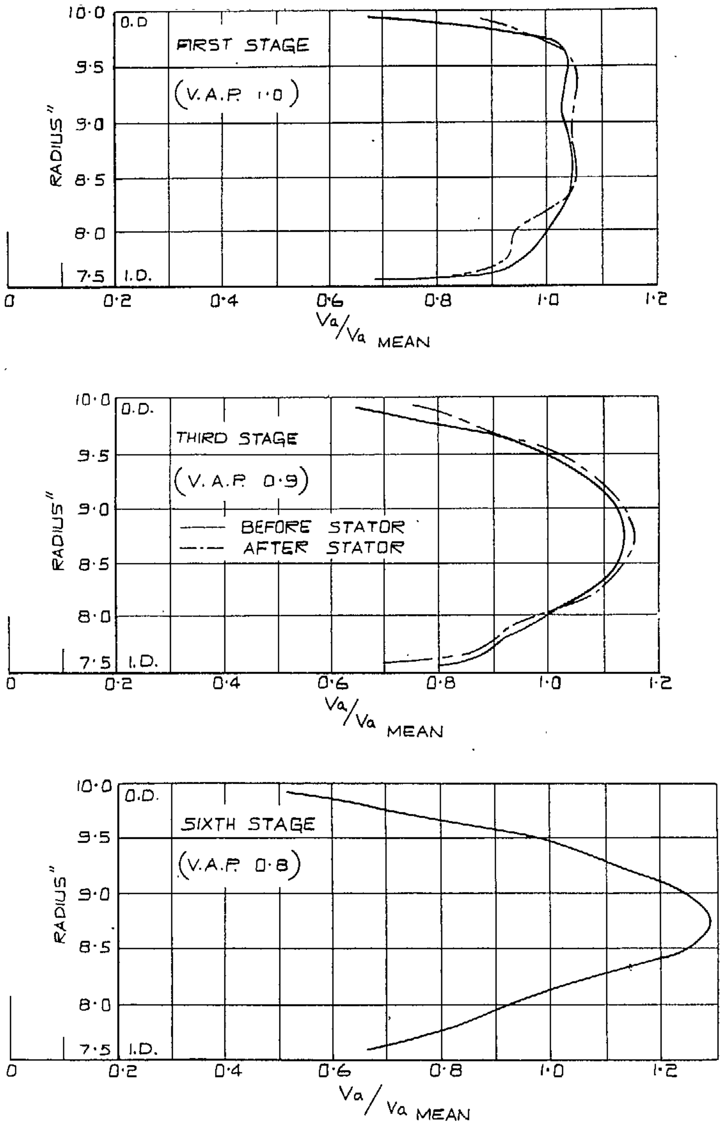

Fig. 9. Axial-velocity distribution of V.A.P. design.

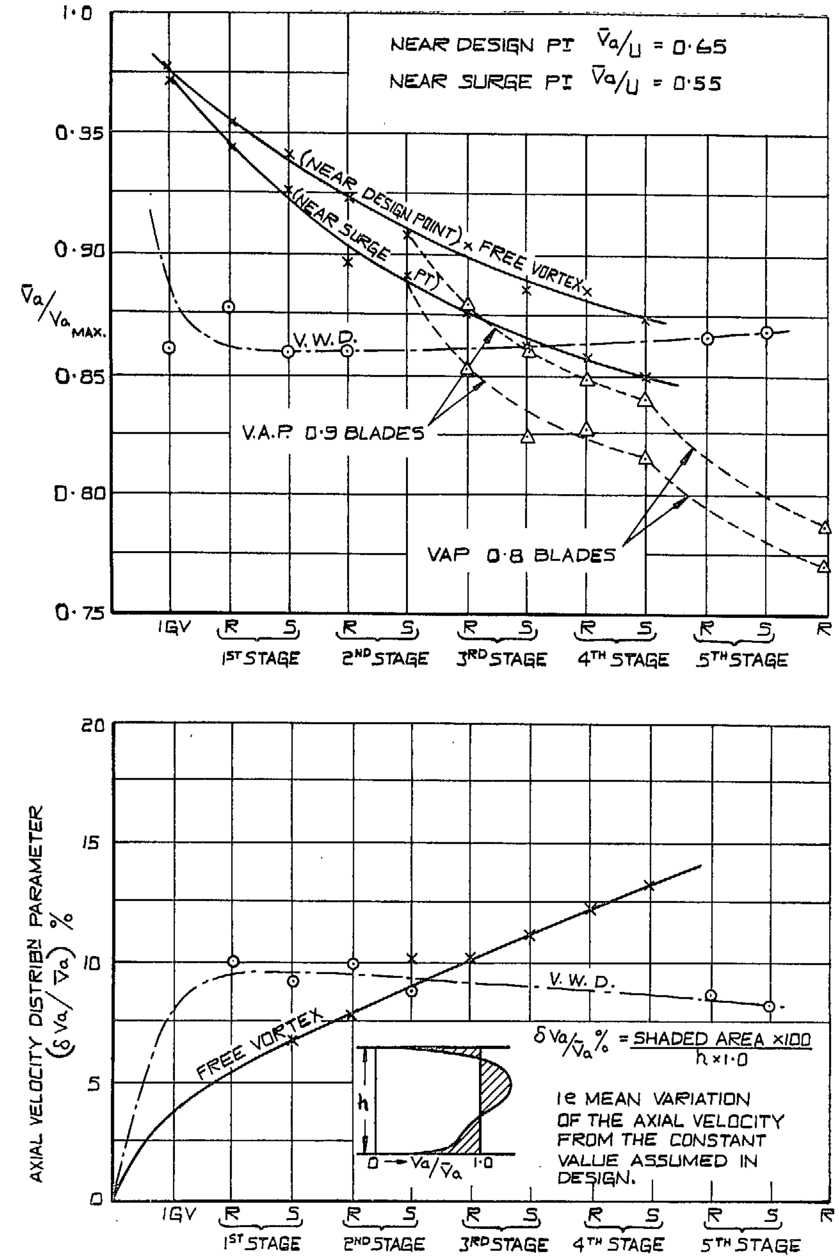

Fig. 10. The deterioration of the axial-velocity profile.

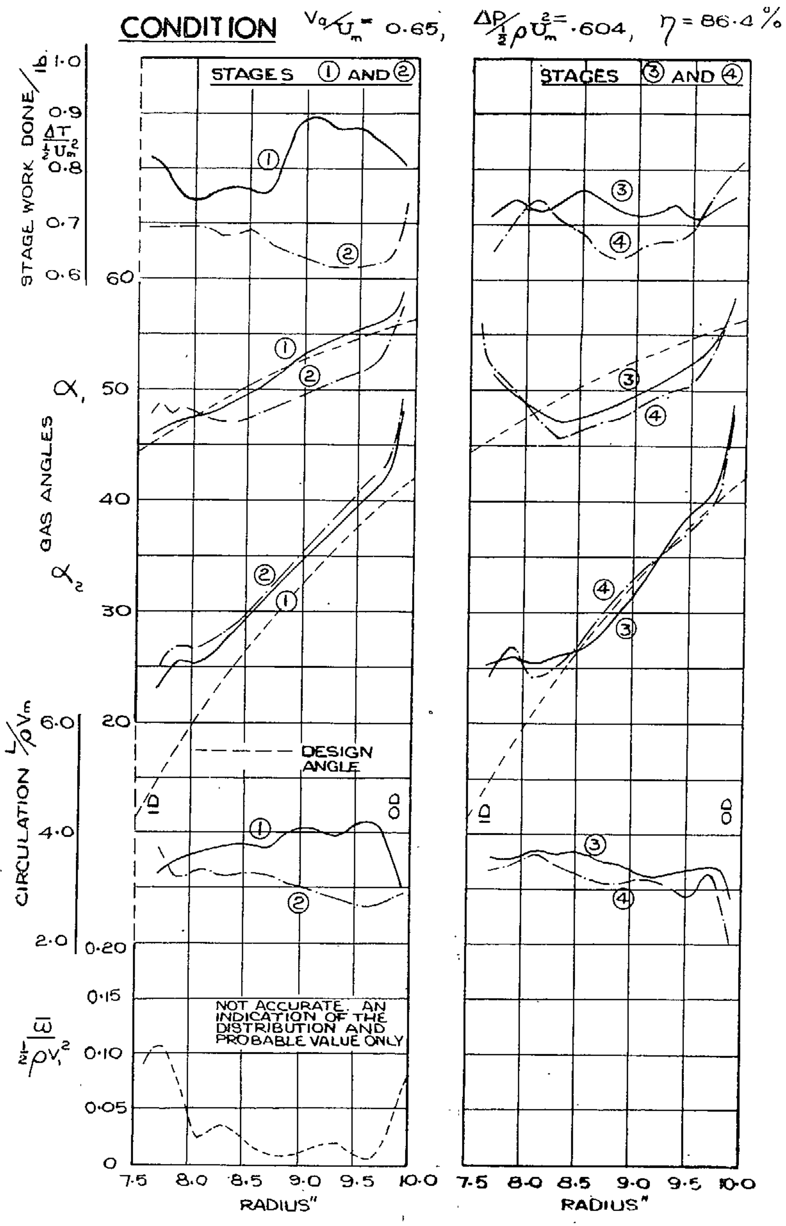

FIG. 11. Flow details in rotor blade rows of Free-Vortex design.

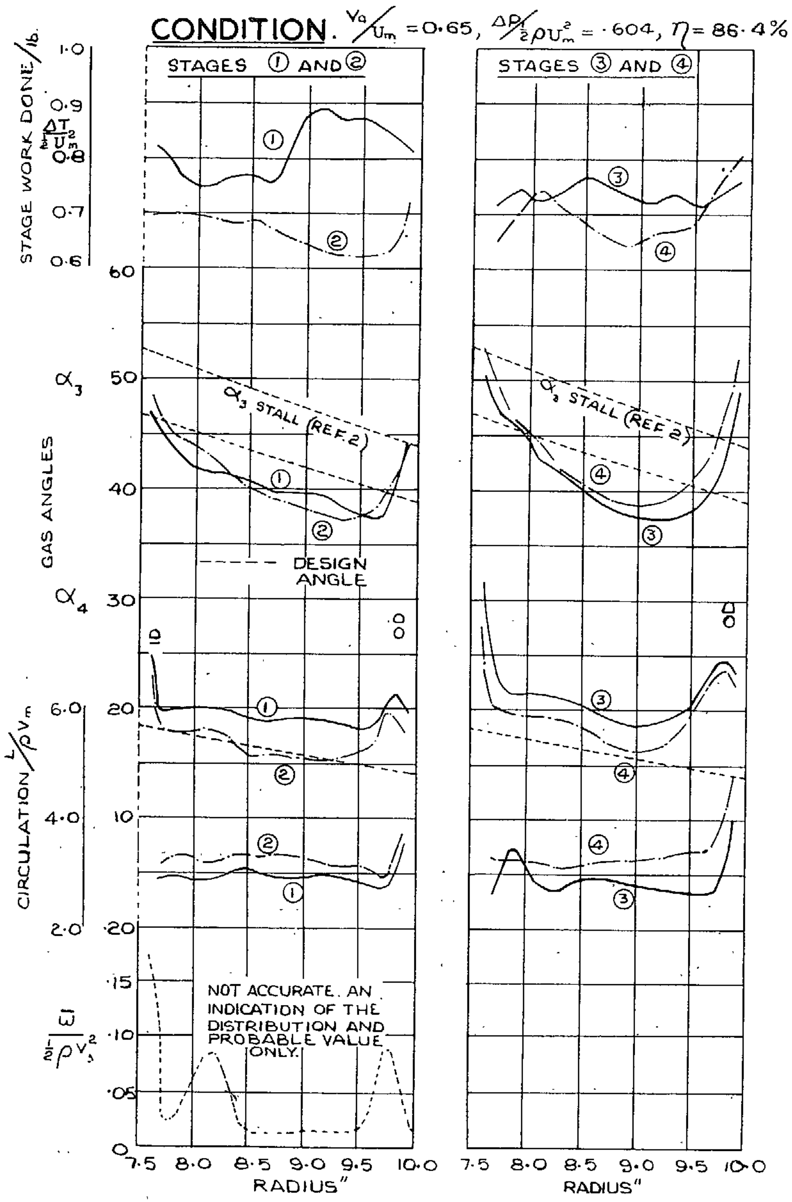

FIG. 12. Flow details in stator blade rows of Free-Vortex design.

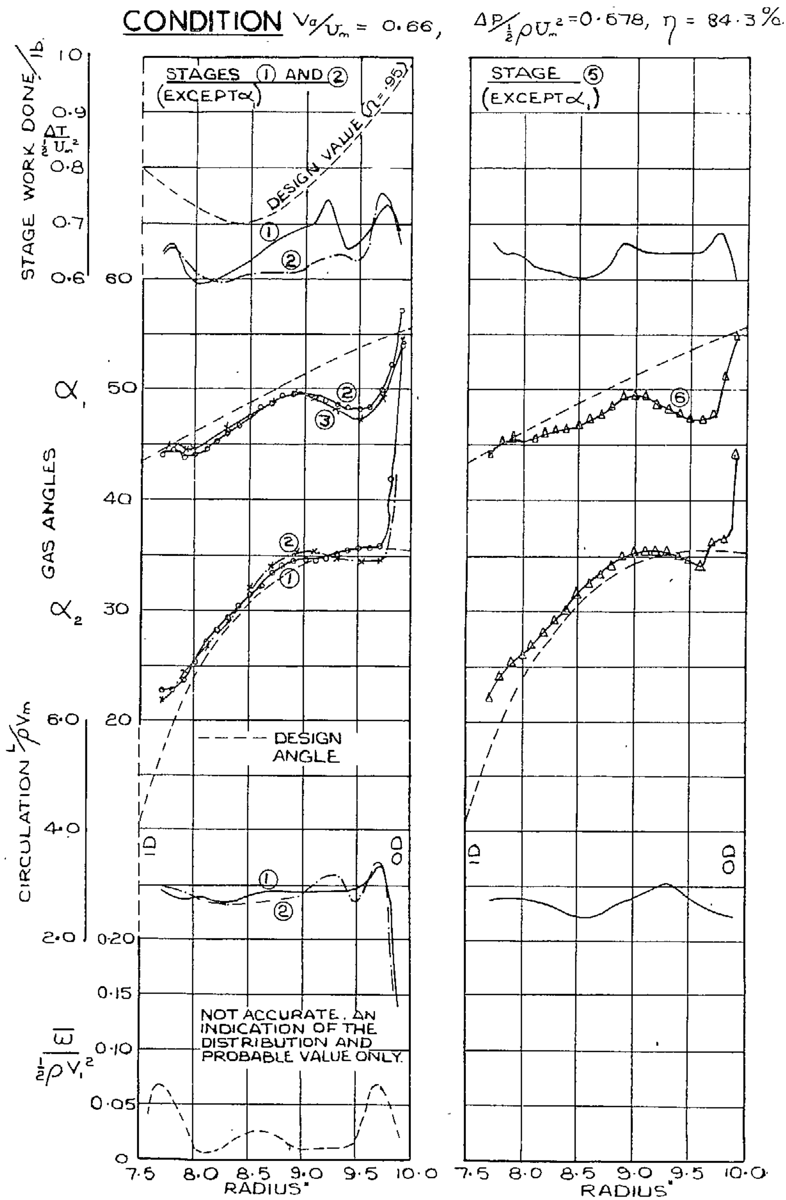

FIG. 13. Flow details in rotor blade rows of V.W.D. design.

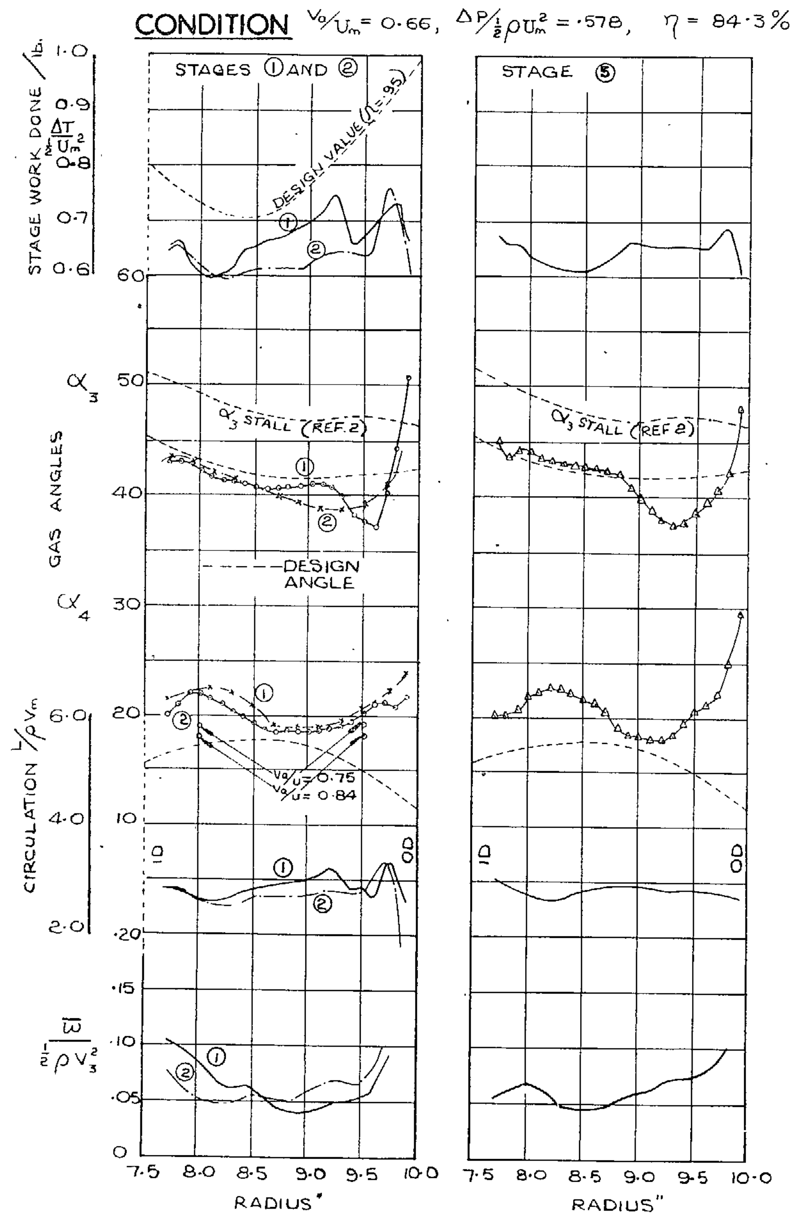

FIG. 14. Flow details in stator blade rows of V.W.D. design.

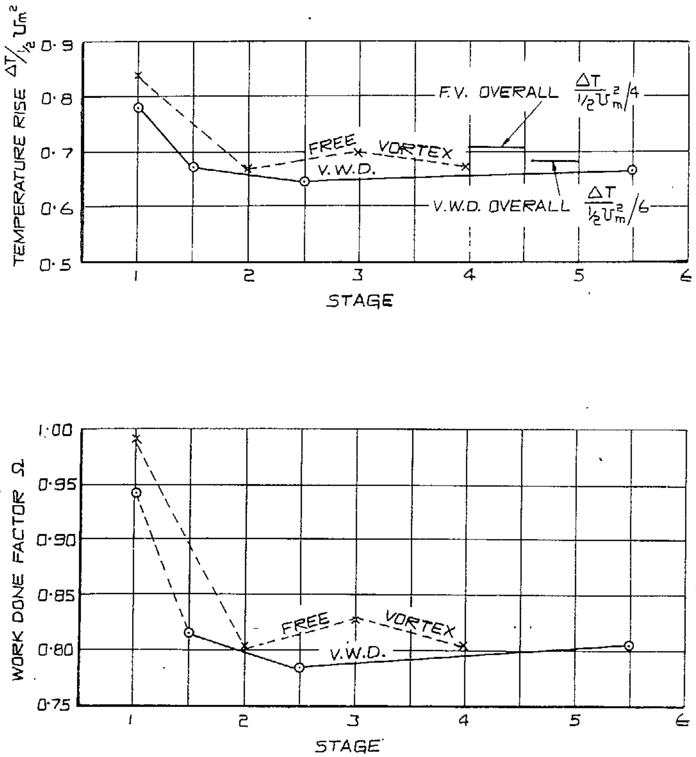

FIG. 15. Variation of work done factor.

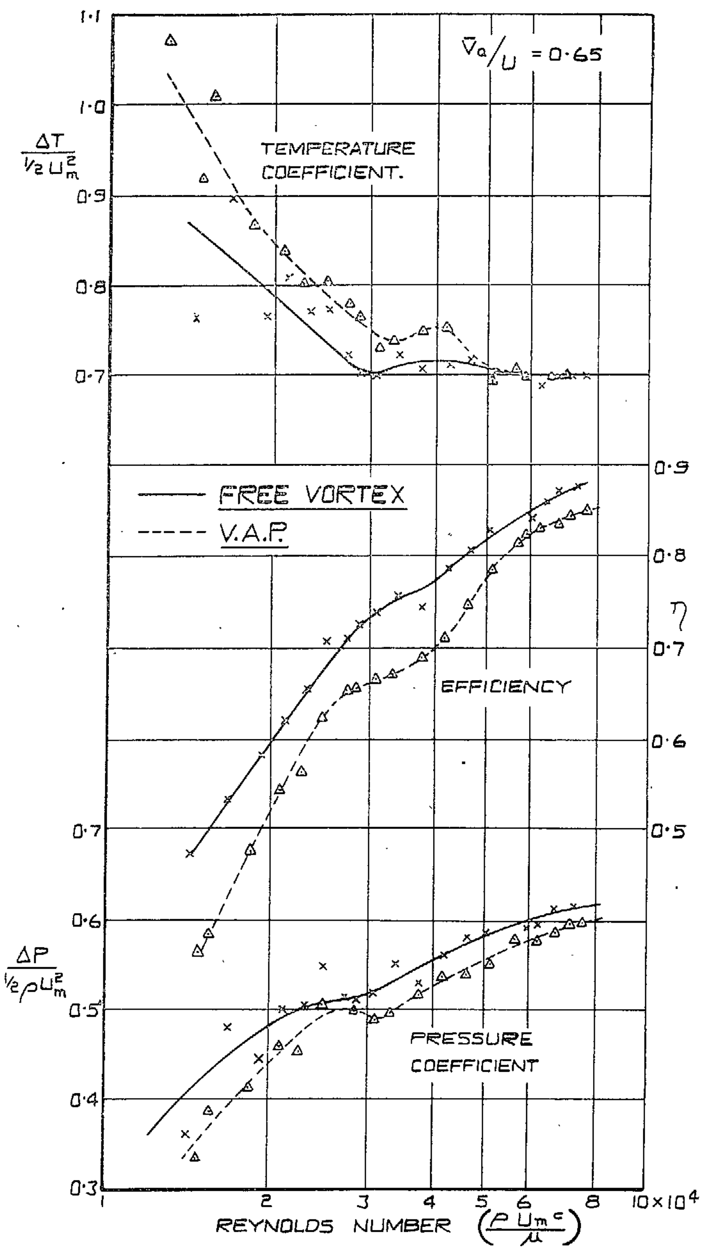

FIG. 16. Reynolds number effects on Free-Vortex and V.A.P. blades.

Printed in Great Britain under the authority of Her Majesty's Stationery Office.
By The Hove Printing Co., Ltd.
(6906) Wt. 18/680. K7. 12/56 H.P.Co. 34-261

Publications of the Aeronautical Research Council

ANNUAL TECHNICAL REPORTS OF THE AERONAUTICAL RESEARCH COUNCIL (BOUND VOLUMES)—

1939 Vol. I. Aerodynamics General, Performance, Airscrews, Engines. 50*s*. (51*s*. 9*d*.)
Vol. II. Stability and Control, Flutter and Vibration, Instruments, Structures, Seaplanes, etc. 63*s*. (64*s*. 9*d*.)

1940 Aero and Hydrodynamics, Aerofoils, Airscrews, Engines, Flutter, Icing, Stability and Control, Structures, and a miscellaneous section. 50*s*. (51*s*. 9*d*.)

1941 Aero and Hydrodynamics, Aerofoils, Airscrews, Engines, Flutter, Stability and Control, Structures. 63*s*. (64*s*. 9*d*.)

1942 Vol. I. Aero and Hydrodynamics, Aerofoils, Airscrews, Engines. 75*s*. (76*s*. 9*d*.)
Vol. II. Noise, Parachutes, Stability and Control, Structures, Vibration, Wind Tunnels. 47*s*. 6*d*. (49*s*. 3*d*.)

1943 Vol. I. Aerodynamics, Aerofoils, Airscrews. 80*s*. (81*s*. 9*d*.)
Vol. II. Engines, Flutter, Materials, Parachutes, Performance, Stability and Control, Structures. 90*s*. (92*s*. 6*d*.)

1944 Vol. I. Aero and Hydrodynamics, Aerofoils, Aircraft, Airscrews, Controls. 84*s*. (86*s*. 3*d*.)
Vol. II. Flutter and Vibration, Materials, Miscellaneous, Navigation, Parachutes, Performance, Plates and Panels, Stability, Structures, Test Equipment, Wind Tunnels. 84*s*. (86*s*. 3*d*.)

1945 Vol. I. Aero and Hydrodynamics, Aerofoils. 130*s*. (132*s*. 6*d*.)
Vol. II. Aircraft, Airscrews, Controls. 130*s*. (132*s*. 6*d*.)
Vol. III. Flutter and Vibration, Instruments, Miscellaneous, Parachutes, Plates and Panels, Propulsion. 130*s*. (132*s*. 3*d*.)
Vol. IV. Stability, Structures, Wind Tunnels, Wind Tunnel Technique. 130*s*. (132*s*. 3*d*.)

ANNUAL REPORTS OF THE AERONAUTICAL RESEARCH COUNCIL—

1937 2*s*. (2*s*. 2*d*.) 1938 1*s*. 6*d*. (1*s*. 8*d*.) 1939–48 3*s*. (3*s*. 3*d*.)

INDEX TO ALL REPORTS AND MEMORANDA PUBLISHED IN THE ANNUAL TECHNICAL REPORTS, AND SEPARATELY—

April, 1950 . . . . . R. & M. No. 2600 2*s*. 6*d*. (2*s*. 8*d*.)

AUTHOR INDEX TO ALL REPORTS AND MEMORANDA OF THE AERONAUTICAL RESEARCH COUNCIL—

1909–January, 1954 . . . . R. & M. No. 2570 15*s*. (15*s*. 6*d*.)

INDEXES TO THE TECHNICAL REPORTS OF THE AERONAUTICAL RESEARCH COUNCIL—

December 1, 1936 — June 30, 1939	R. & M. No. 1850	1*s*. 3*d*. (1*s*. 5*d*.)
July 1, 1939 — June 30, 1945	R. & M. No. 1950	1*s*. (1*s*. 2*d*.)
July 1, 1945 — June 30, 1946	R. & M. No. 2050	1*s*. (1*s*. 2*d*.)
July 1, 1946 — December 31, 1946	R. & M. No. 2150	1*s*. 3*d*. (1*s*. 5*d*.)
January 1, 1947 — June 30, 1947	R. & M. No. 2250	1*s*. 3*d*. (1*s*. 5*d*.)

PUBLISHED REPORTS AND MEMORANDA OF THE AERONAUTICAL RESEARCH COUNCIL—

Between Nos. 2251–2349	R. & M. No. 2350	1*s*. 9*d*. (1*s*. 11*d*.)
Between Nos. 2351–2449	R. & M. No. 2450	2*s*. (2*s*. 2*d*.)
Between Nos. 2451–2549	R. & M. No. 2550	2*s*. 6*d*. (2*s*. 8*d*.)
Between Nos. 2551–2649	R. & M. No. 2650	2*s*. 6*d*. (2*s*. 8*d*.)

Prices in brackets include postage

HER MAJESTY'S STATIONERY OFFICE

York House, Kingsway, London, W.C.2; 423 Oxford Street, London, W.1 (Post Orders: P.O. Box 569, London, S.E.1); 13a Castle Street, Edinburgh 2; 39 King Street, Manchester 2; 2 Edmund Street, Birmingham 3; 109 St. Mary Street, Cardiff; Tower Lane, Bristol 1; 80 Chichester Street, Belfast *or through any bookseller.*

S.O. Code No. 23-2929